Chapter 22
Bounded Error Identification of Hammerstein Systems with Backlash

Vito Cerone, Dario Piga, and Diego Regruto

22.1 Introduction

Actuators and sensors commonly used in control systems may exhibit a variety of nonlinear behaviours that may be responsible for undesirable phenomena such as delays and oscillations, which may severely limit both the static and the dynamic performance of the system under control (see, *e.g.*, [22]). In particular, one of the most relevant nonlinearities affecting the performance of industrial machines is the backlash (see Figure 22.1), which commonly occurs in mechanical, hydraulic and magnetic components like bearings, gears and impact dampers (see, *e.g.*, [17]). This nonlinearity, which can be classified as dynamic (*i.e.*, with memory) and hard (*i.e.* non-differentiable), may arise from unavoidable manufacturing tolerances or sometimes may be deliberately incorporated into the system in order to describe lubrication and thermal expansion effects [3]. The interested reader is referred to [22] for real-life examples of systems with either input or output backlash nonlinearities.

In order to cope with the limitations caused by the presence of backlash, either robust or adaptive control techniques can be successfully employed (see, *e.g.*, [7], and [21] respectively), which, on the other hand, require the characterisation of the nonlinear dynamic block. Few contributions can be found in literature on the iden-

Vito Cerone
Dipartimento di Automatica e Informatica, Politecnico di Torino,
corso Duca degli Abruzzi 24, 10129 Torino, Italy
e-mail: vito.cerone@polito.it

Dario Piga
Dipartimento di Automatica e Informatica, Politecnico di Torino,
corso Duca degli Abruzzi 24, 10129 Torino, Italy
e-mail: dario.piga@polito.it

Diego Regruto
Dipartimento di Automatica e Informatica, Politecnico di Torino,
corso Duca degli Abruzzi 24, 10129 Torino, Italy
e-mail: diego.regruto@polito.it

F. Giri & E.-W. Bai (Eds.): Block-oriented Nonlinear System Identification, LNCIS 410, pp. 367–382.
springerlink.com

tification of systems with input backlash. An input-holding scheme is exploited in [20] to compute the system parameters estimates by solving least squares problems, while a separable least squares approach is discussed in [1]. In [8] a consistent estimator, based on careful selection of the system parametrisation and the input signal, is presented, whereas an iterative algorithm relying on a newly proposed model for the backlash nonlinearity is discussed in [23].

Although the most common assumption in system identification is that measurement errors are statistically described, a worthwhile alternative is the bounded-errors or set-membership characterisation, where uncertainties are assumed to belong to a given set. In this context all parameters consistent with measurements, error bounds and the assumed model structure are feasible solutions of the identification problem. The interested reader can refer to survey papers [15, 24] and book [14] for a thorough presentation of the main theoretical basis.

In this chapter, the procedure for the identification of linear systems with input backlash presented in [6] is reviewed and improved. More specifically, the problem of bounding the parameters of a stable, single-input single-output (SISO) discrete time linear system with unknown input backlash (see Figure 22.2) in the presence of bounded output measurement error is considered, under the common assumption that the inner signal $x(t)$ is not supposed to be measurable.

The chapter is organised as follows. Section 22.2 is devoted to the problem formulation. In Section 22.3, parameters of the nonlinear block are tightly bounded using input-output data from the steady-state response of the system to a collection of square wave inputs. Then, in Section 22.4, through a dynamic experiment, for all u_t belonging to a suitable pseudo random binary signal (PRBS) sequence $\{u_t\}$, we compute tight bounds on the inner signal, which are used to bound the parameters of the linear part together with noisy output measurements. Recently proposed relaxation techniques based on linear matrix inequalities (LMIs) are exploited in the identification of the linear block parameters, providing a significant improvement over the algorithm proposed in [6]. A simulated example is reported in Section 22.5.

22.2 Problem Formulation

Let us consider the Hammerstein system depicted in Figure 22.2, where the nonlinear block that transforms the input signal u_t into the unmeasurable inner variable x_t is a backlash described by (see, *e.g.*, [22])

$$x_t = \begin{cases} m_l(u_t + c_l) & \text{for } u_t \leq z_l, \\ m_r(u_t - c_r) & \text{for } u_t \geq z_r, \\ x_{t-1} & \text{for } z_l < u_t < z_r, \end{cases} \tag{22.1}$$

where $m_l > 0$, $m_r > 0$, $c_l > 0$, $c_r > 0$ are constant parameters characterising the backlash and

$$z_l \doteq \frac{x_{t-1}}{m_l} - c_l, \quad z_r \doteq \frac{x_{t-1}}{m_r} + c_r, \tag{22.2}$$

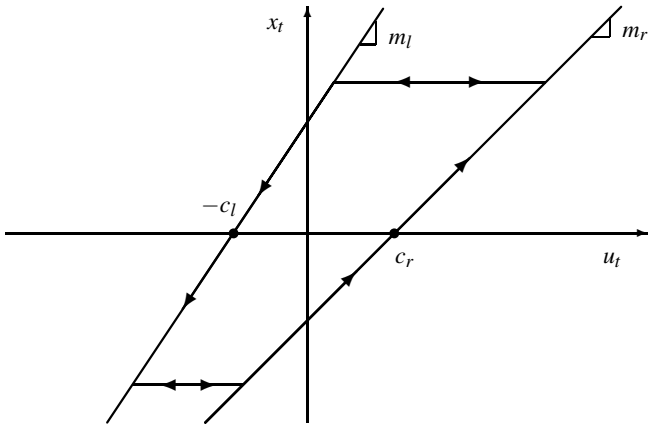

Fig. 22.1: Backlash characteristic

are the u-axis values of the intersections between the two lines with slopes m_l and m_r and the horizontal inner segment containing x_{t-1}. The backlash characteristic is depicted in Figure 22.1.

The block that maps x_t into the noise-free output w_t is a discrete-time linear dynamic SISO system defined by

$$w_t = \mathscr{G}(q^{-1})x_t = \frac{\mathscr{B}(q^{-1})}{\mathscr{A}(q^{-1})}x_t, \tag{22.3}$$

where $\mathscr{A}(q^{-1}) = 1 + a_1 q^{-1} + \ldots + a_{na} q^{-na}$ and $\mathscr{B}(q^{-1}) = b_0 + b_1 q^{-1} + \ldots + b_{nb} q^{-nb}$ are polynomials in the backward shift operator q^{-1}, $(q^{-1} w_t = w_{t-1})$. Furthermore, the following common assumptions are made:

A1 the linear system is asymptotically stable (see, *e.g.*, [10, 11, 12, 19, 20]);
A2 the steady-state gain of the linear block is not equal to zero (see, *e.g.*, [11, 12, 20]);
A3 a rough upper bound of the settling time is available (see, *e.g.*, [9]).

As ordinarily assumed in block-oriented nonlinear system identification, the inner signal x_t is not supposed to be measurable. Therefore, identification of the Hammerstein system described by (22.1) - (22.3) relies only on input-output data. Here, we assume that the input signal u_t is exactly known, while measurements y_t of output w_t are corrupted by bounded additive noise according to

$$y_t = w_t + \eta_t, \tag{22.4}$$

where

$$| \eta_t | \leq \Delta \eta_t. \tag{22.5}$$

Let $\gamma \in \mathbb{R}^4$ and $\theta \in \mathbb{R}^p$ be the unknown parameter vectors to be estimated, defined as

$$\gamma^T \doteq [\ \gamma_1 \ \ \gamma_2 \ \ \gamma_3 \ \ \gamma_4\ ] = [\ m_l \ \ c_l \ \ m_r \ \ c_r\ ], \tag{22.6}$$

$$\theta^T \doteq [\ a_1 \ \ \ldots \ \ a_{na} \ \ b_0 \ \ b_1 \ \ \ldots b_{nb}\ ], \tag{22.7}$$

where $na+nb+1=p$. It is worth noting that the parametrisation of the structure depicted in Figure 22.2 is not unique. In fact, given the pair of subsystems $\tilde{\mathscr{G}}(q^{-1})$, $\tilde{\mathscr{N}}(u_t,\tilde{\gamma})$, any Hammerstein system (see Figure 22.2) with $\mathscr{G}(q^{-1}) = \alpha^{-1}\tilde{\mathscr{G}}(q^{-1})$ and $\mathscr{N}(w_t,\gamma) = \tilde{\mathscr{N}}(w_t,\alpha\tilde{\gamma})$ provides the same input-output behaviour for any nonzero and finite constant $\alpha \in \mathbb{R}$. In order to get a unique parametrisation, in this work we assume that the steady-state gain g of the linear block $\mathscr{G}(q^{-1})$ be one, that is:

$$g = \frac{\sum_{j=0}^{nb} b_j}{1+\sum_{i=1}^{na} a_i} = 1. \tag{22.8}$$

In the next sections we describe a two-stage procedure for deriving lower and upper bounds of parameters γ and θ, consistently with the assumed model structure, given measurements and uncertainty bounds.

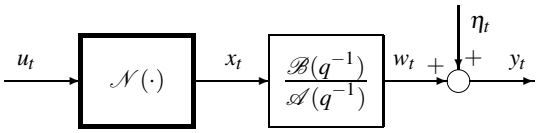

Fig. 22.2: Hammerstein system with backlash

22.3 Assessment of Tight Bounds on the Nonlinear Static Block Parameters

In this section we describe the first step of the proposed identification procedure where steady-state operating conditions are exploited to bound the parameters of the backlash. We apply to the system a set of square wave inputs with M different amplitudes and collect $2M$ steady-state values of the noisy output. More precisely, for each value of the input square wave amplitude, one steady-state output sample is collected on the positive half-wave of the input and one steady-state output measurement is collected on the negative half-wave. Because the backlash deadzone is unknown, the input amplitude must be chosen as large as to guarantee that the output shows any nonzero response. By combining Eqs. (22.1), (22.3), (22.4) and (22.8) under assumptions A1, A2 and A3 stated in Section 22.2, we obtain the following input-output description of the system in Figure 22.2 in steady-state operating conditions:

$$\begin{aligned} \bar{w}_i &= m_r(\bar{u}_i - c_r) \quad \text{for } \bar{u}_i \geq \frac{\bar{w}_{i-1}}{m_r} + c_r, \\ \bar{y}_i &= \bar{w}_i + \bar{\eta}_i, \qquad i = 1,\ldots,M; \end{aligned} \tag{22.9}$$

$$\begin{aligned} \bar{w}_j &= m_l(\bar{u}_j + c_l) \quad \text{for } \bar{u}_j \leq \frac{\bar{w}_{j-1}}{m_l} - c_l, \\ \bar{y}_j &= \bar{w}_j + \bar{\eta}_j, \qquad j = 1,\ldots,M; \end{aligned} \tag{22.10}$$

where the triplets $\{\bar{u}_i, \bar{y}_i, \bar{\eta}_i\}$ and $\{\bar{u}_j, \bar{y}_j, \bar{\eta}_j\}$ are collections of steady-state values of the known input signal, output observation and measurement error taken during the positive and the negative square wave respectively. As can be noted, Eqs. (22.9) and (22.10) depend only on the backlash parameters, thus the identification of γ can be carried out leaving aside the dynamics of the linear block. A block diagram description of Equation (22.10) is depicted in Figure 22.3; an analogous schematic representation also hold for Equation (22.9). Because (22.9) depends only on the right side backlash parameters m_r and c_r, while (22.10) involves only m_l and c_l, the overall feasible parameter region of the backlash can be written as the Cartesian product of two sets, that is

$$\mathscr{D}_\gamma \doteq \mathscr{D}_\gamma^r \times \mathscr{D}_\gamma^l, \tag{22.11}$$

where

$$\mathscr{D}_\gamma^r \doteq \left\{ (m_r, c_r) \in \mathbb{R}_+^2 : \bar{y}_i = m_r(\bar{u}_i - c_r) + \bar{\eta}_i, \mid \bar{\eta}_i \mid \leq \Delta\bar{\eta}_i;\ i = 1,\ldots,M \right\}, \tag{22.12}$$

$$\mathscr{D}_\gamma^l \doteq \left\{ (m_l, c_l) \in \mathbb{R}_+^2 : \bar{y}_j = m_l(\bar{u}_j + c_l) + \bar{\eta}_j, \mid \bar{\eta}_j \mid \leq \Delta\bar{\eta}_j;\ j = 1,\ldots,M \right\}, \tag{22.13}$$

$\{\Delta\bar{\eta}_i\}$ and $\{\Delta\bar{\eta}_j\}$ are the sequences of bounds on measurements uncertainty.

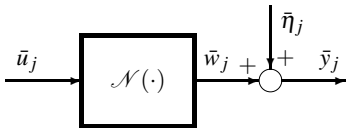

Fig. 22.3: Hammerstein system with backlash in steady-state operating conditions

Remark 22.1. $\mathscr{D}_\gamma^r$ and $\mathscr{D}_\gamma^l$ are 2-dimensional disjoint sets lying on the $(m_r, c_r)-$plane and the $(m_l, c_l)-$plane respectively, which means that they can be handled separately. It is worth noting that $\mathscr{D}_\gamma^r$ and $\mathscr{D}_\gamma^l$ are 2-dimensional sets enjoying the same topological features and the same mathematical properties. Therefore, the results derived in the rest of the paper for one of the two sets, say $\mathscr{D}_\gamma^l$, also hold for the other set ($\mathscr{D}_\gamma^r$).

Remark 22.2. Note that $\mathscr{D}_\gamma^r$ and $\mathscr{D}_\gamma^l$ are bounded sets as far as at least two measurements with different input amplitude are collected.

An exact description of the feasible parameter set $\mathscr{D}_\gamma^l$ in terms of edges and vertices is presented below together with an orthotopic outer-bounding set providing tight parameter uncertainty intervals. Introductory definitions and preliminary results are first given.

22.3.1 Definitions and Preliminary Results

Definition 22.1. Let $h_l^+(\overline{u}_j)$ and $h_l^-(\overline{u}_j)$ be the constraints boundaries defining the FPS $\mathscr{D}_\gamma^l$ corresponding to the j-th sets of data:

$$h_l^+(\overline{u}_j) \doteq \left\{(m_l,c_l)\in\mathbb{R}_+^2 : \overline{y}_j+\Delta\eta_j = m_l(\overline{u}_j-c_l)\right\}, \tag{22.14}$$

$$h_l^-(\overline{u}_j) \doteq \left\{(m_l,c_l)\in\mathbb{R}_+^2 : \overline{y}_j-\Delta\eta_s = m_l(\overline{u}_j-c_l)\right\}. \tag{22.15}$$

Definition 22.2. Boundary of $\mathscr{D}_\gamma^l \doteq \partial\mathscr{D}_\gamma^l$.

Definition 22.3. The constraints boundaries $h_l^+(\overline{u}_j)$ and $h_l^-(\overline{u}_j)$ are said to be active if their intersections with $\partial\mathscr{D}_\gamma^l$ is not the empty set:

$$h_l^+(\overline{u}_j)\bigcap\partial\mathscr{D}_\gamma^l \neq \emptyset \Longleftrightarrow h_l^+(\overline{u}_j) \textit{ is active.} \tag{22.16}$$

$$h_l^-(\overline{u}_j)\bigcap\partial\mathscr{D}_\gamma^l \neq \emptyset \Longleftrightarrow h_l^-(\overline{u}_j) \textit{ is active.} \tag{22.17}$$

Remark 22.3. The constraints boundaries $h_l^+(\overline{u}_j)$ and $h_l^-(\overline{u}_j)$ may either intersect $\partial\mathscr{D}_\gamma^l$ or be external to $\mathscr{D}_\gamma^l$.

Definition 22.4 (Edges of $\mathscr{D}_\gamma^l$).

$$\tilde{h}_l^+(\overline{u}_j) \doteq h_l^+(\overline{u}_j)\bigcap\mathscr{D}_\gamma^l = \left\{m_l,c_l\in\mathscr{D}_\gamma^l : \overline{y}_j+\Delta\eta_j = m_l(\overline{u}_j-c_l)\right\}, \tag{22.18}$$

$$\tilde{h}_l^-(\overline{u}_j) \doteq h_l^-(\overline{u}_j)\bigcap\mathscr{D}_\gamma^l = \left\{m_l,c_l\in\mathscr{D}_\gamma^l : \overline{y}_s-\Delta\eta_j = m_l(\overline{u}_j-c_l)\right\}. \tag{22.19}$$

Definition 22.5 (Constraints intersections). The set of all pairs $(m_l,c_l)\in\mathbb{R}_+^2$ where intersections among the constraints occur is

$$\begin{aligned}\mathscr{I}_\gamma^l \doteq \Big\{&(m_l,c_l)\in\mathbb{R}_+^2 : \{h_r^+(\overline{u}_\rho),h_r^-(\overline{u}_\rho)\}\bigcap\{h_r^+(\overline{u}_\sigma),h_r^-(\overline{u}_\sigma)\}\neq\emptyset;\\ &\rho,\sigma=1,\ldots,M;\rho\neq\sigma\Big\}.\end{aligned} \tag{22.20}$$

Definition 22.6 (Vertices of $\mathscr{D}_\gamma^l$). The set of all vertices of $\mathscr{D}_\gamma^l$ is defined as the set of all intersection couples belonging to the feasible parameter set $\mathscr{D}_\gamma^l$:

$$\mathscr{V}(\mathscr{D}_\gamma^l) \doteq \mathscr{I}_\gamma^l\bigcap\mathscr{D}_\gamma^l. \tag{22.21}$$

22.3.2 Exact Description of $\mathscr{D}_\gamma^l$

An exact description of $\mathscr{D}_\gamma^l$ can be given in terms of edges, each one being described, from a practical point of view, as a subset of an active constraint lying between two vertices. An effective procedure for deriving active constraints, vertices and edges of $\mathscr{D}_\gamma^l$ is reported in the Appendix.

22.3.3 Tight Orthotope Description of $\mathscr{D}_\gamma^l$

Unfortunately, the exact description of $\mathscr{D}_\gamma^l$ provided by edges could be not so easy to handle. A somewhat more practical, although approximate, description can be obtained by computing the following tight orthotope outer-bounding set $\mathscr{P}_\gamma^l$ containing $\mathscr{D}_\gamma^l$:

$$\mathscr{P}_\gamma^l \doteq \left\{\gamma \in \mathbb{R}_+^2 : \gamma_j = \gamma_j^c + \delta\gamma_j, \mid \delta\gamma_j \mid \leq \Delta\gamma_j, j = 1,2\right\}, \tag{22.22}$$

where

$$\gamma_j{}^c \doteq \frac{\gamma_j^{min} + \gamma_j^{max}}{2}, \qquad \Delta\gamma_j \doteq \frac{(\gamma_j^{max} - \gamma_j^{min})}{2}, \tag{22.23}$$

$$\gamma_j^{min} \doteq \min_{\gamma \in \mathscr{D}_\gamma^l} \gamma_j, \quad \gamma_j^{max} \doteq \max_{\gamma \in \mathscr{D}_\gamma^l} \gamma_j. \tag{22.24}$$

Because the constraints defining $\mathscr{D}_\gamma^l$ are nonconvex in m_l and c_l, standard nonlinear optimisation tools (gradient method, Newton method, *etc.*) cannot be used to solve problems (22.24) since they can trap in local minima, which may result arbitrary far from the global one. Thus, parameter uncertainty intervals obtained using these tools are not guaranteed to contain the true unknown parameters, which is a key requirement of any bounded-error identification method. Global optimal solutions to problems (22.24) can be computed thanks to the result reported below.

Proposition 22.1. *The global optimal solutions to problems* (22.24) *occur on the vertices of* $\mathscr{D}_\gamma^l$.

Proof. First (i) we notice that each level curve of functionals (22.24) — parallel lines to m_l-axis and c_l-axis respectively — intersect the constraint boundaries (22.14) and (22.15) only once. Next, (ii) objective functions in (22.24) are monotone in $\mathscr{D}_\gamma^l$, which implies that the optimal solution lies on the boundary of $\mathscr{D}_\gamma^l$. Thanks to (i) the optimal value cannot lie on one edge between two vertices: if that was true, it would mean that there is a suboptimal value where the functional intersect the edge twice: that would contradict (i). Then the global optimal solutions of problems (22.24) can only occur on the vertices of $\mathscr{D}_\gamma^l$. □

Remark 22.4. Given the set of vertices $\mathscr{V}(\mathscr{D}_\gamma^l)$ computed via Algorithm 22.1 reported in the Appendix, evaluation of (22.24) is an easy task because it only requires the computation of (a) the objective functions on a set of at most $4M$ points and (b) the maximum over a set of real-valued elements.

22.4 Bounding the Parameters of the Linear Dynamic Model

In the second stage of the presented procedure, parameters bounds of the linear dynamic part are computed, using a PRBS input $\{u_t\}$ taking values $\pm u^\star$, with $u^\star > 0$. Thanks to its properties, this kind of input sequence has been successfully used to identify linear dynamic systems (see, *e.g.*, [13, 18]) while, in general, it is inappropriate for the identification of nonlinear systems (see, *e.g.*, [1, 16]). However, as shown in [2], a PRBS input can be effectively employed to decouple the linear and the nonlinear parts in the identification of Hammerstein models with a static nonlinearity. In this chapter we show that the use of a PRBS sequence is profitable for the identification of linear system with input backlash. The key idea underlying the choice of the input sequence $\{u_t\}$ is based on the following result.

Result 1. *Let us consider a PRBS input $\{u_t\}$ whose levels are $\pm u^\star$. If $u^\star > c_r$ and $-u^\star < -c_l$, then the output sequence $\{x_t\}$ of the backlash described by* (22.1) *is still a PRBS with levels $\bar{x}^\star = m_r(u^\star - c_r)$, $\underline{x}^\star = m_l(u^\star - c_l)$.*

Proof. The proof of Result 1 follows from the backlash mathematical model (22.1) assuming $u = u^\star$ with $u^\star > c_r$ and $-u^\star < -c_l$. □

From Result 1, it can be noted that the choice of suitable PRBS input levels $\pm u^\star$ depends on the unknown parameters c_r and c_l, which are bounded in the first stage of the presented procedure. Therefore, in order to satisfy hypotheses of Result 1, values of $u^\star$, such that $u^\star > c_r^{max}$ and $-u^\star < -c_l^{max}$, are chosen.

Given the exact description of $\mathscr{D}_\gamma^r$ and $\mathscr{D}_\gamma^l$, tight bounds on the amplitudes $\bar{x}^\star$ and $\underline{x}^\star$ of unmeasurable inner signal x_t can be defined as

$$\begin{aligned} \bar{x}^{\star min} &\doteq \min_{m_r, c_r \in \mathscr{D}_\gamma^r} m_r(u^\star - c_r), \quad \text{for } u^\star \geq c_r^{max}, \\ \bar{x}^{\star max} &\doteq \max_{m_r, c_r \in \mathscr{D}_\gamma^r} m_r(u^\star - c_r), \quad \text{for } u^\star \geq c_r^{max}, \end{aligned} \tag{22.25}$$

$$\begin{aligned} \underline{x}^{\star min} &\doteq \min_{m_l, c_l \in \mathscr{D}_\gamma^l} m_l(u^\star + c_l), \quad \text{for } -u^\star \leq -c_l^{max}, \\ \underline{x}^{\star max} &\doteq \max_{m_l, c_l \in \mathscr{D}_\gamma^l} m_(u^\star + c_l), \quad \text{for } -u^\star \leq -c_l^{max}. \end{aligned} \tag{22.26}$$

Computation of bounds in (22.25) and (22.26) requires, at least in principle, the solution to two nonconvex optimisation problems with two variables and $4M$ nonlinear inequality constraints. Thanks to Proposition 22.2 reported below, the global optimal solution is guaranteed to be achieved.

Definition 22.7. Let us define the x-level curve of the objective function of problem (22.25) as

$$g_r(u^\star, x) \doteq \left\{ (m_r, c_r) \in \mathbb{R}^2_+ : x = m_r(u^\star - c_r) \right\}, \tag{22.27}$$

and the x-level curve of the objective function of problem (22.26) as

$$g_l(u^\star, x) \doteq \left\{ (m_l, c_l) \in \mathbb{R}^2_+ : x = m_l(-u^\star + c_l) \right\}. \tag{22.28}$$

Proposition 22.2. *The global optimal solutions to problems* (22.25) *and* (22.26) *occur on the vertices of $\mathscr{D}^r_\gamma$ and $\mathscr{D}^l_\gamma$, respectively.*

Proof. First (i) we notice that each x-level curve $g_l(u^\star, x)$ intersect each constraint boundary in (22.14) and (22.15) only once. Next, (ii) the objective function $x = m_l(-u^\star + c_l)$ is a monotone function in $\mathscr{D}^l_\gamma$, which implies that the optimal solution lies on the boundary of $\mathscr{D}^l_\gamma$. Thanks to (i) the optimal value cannot lie on an edge between two vertices: if that was true, it would mean that there is a suboptimal value where the functional intersect the edge twice: that would contradict (i). Then the global optimal solutions to problems (22.26) can only occur on the vertices of $\mathscr{D}^l_\gamma$. Similar considerations apply to the right side of the backlash. □

By defining the central estimate $\bar{x}^c_t$ of $\bar{x}^\star_t$ and the uncertainty bound $\Delta\bar{x}^\star_t$ as

$$\bar{x}^c_t \doteq \frac{\bar{x}^{\star min} + \bar{x}^{\star max}}{2}, \qquad \Delta\bar{x}_t \doteq \frac{\bar{x}^{\star max} - \bar{x}^{\star min}}{2}, \tag{22.29}$$

as well as the central estimate $\underline{x}^c_t$ and the uncertainty bound $\Delta\underline{x}_t$ of $\underline{x}^\star_t$ as

$$\underline{x}^c_t \doteq \frac{\underline{x}^{\star min} + \underline{x}^{\star max}}{2}, \qquad \Delta\underline{x}_t \doteq \frac{\underline{x}^{\star max} - \underline{x}^{\star min}}{2}, \tag{22.30}$$

the following relation can be established between the unknown inner signals x_t and the corresponding central value x^c_t:

$$x^c_t = x_t + \delta x_t, \quad |\, \delta x_t \,| \leq \Delta x_t, \tag{22.31}$$

where

$$x^c_t = \bar{x}^c_t, \quad \Delta x_t = \Delta\bar{x}_t \quad \text{if } u_t = u^\star, \tag{22.32}$$

$$x^c_t = \underline{x}^c_t, \quad \Delta x_t = \Delta\underline{x}_t \quad \text{if } u_t = -u^\star. \tag{22.33}$$

Given the uncertain inner sequence $\{x^c_t\}$ and the noise-corrupted output sequence $\{y_t\}$, the problem of parameters bounds evaluation of the linear system can be formulated in the framework of bounded errors-in-variables (EIV) as shown in Figure 22.4, *i.e.* the identification of linear dynamic models where both the input and the output are affected by bounded uncertainties.

The exact description of the feasible parameter region $\mathscr{D}_\theta$ for the linear system, *i.e.* the set of all linear model parameters θ consistent with the assumed model structure, input and output signals x_t and y_t and error bounds Δx_t and $\Delta\eta_t$, is

$$\begin{aligned}\mathscr{D}_\theta \doteq \Big\{ \theta \in \mathbb{R}^p : & \mathscr{A}(q^{-1})(y_t - \eta_t) = \mathscr{B}(q^{-1})(x_t^c - \delta x_t); \\ & g = 1; \mid \eta_t \mid \leq \Delta\eta_t; \mid \delta x_t \mid \leq \Delta x_t; t = 1, \ldots, N \Big\},\end{aligned} \tag{22.34}$$

where N is the length of data sequence and $g = 1$ accounts for condition (22.8) on the steady-state gain. The parameter uncertainty intervals defined as

$$PUI_j \doteq \left[\underline{\theta}_j, \overline{\theta}_j\right], \tag{22.35}$$

where

$$\underline{\theta}_j \doteq \min_{\theta \in \mathscr{D}_\theta} \theta_j, \tag{22.36}$$

$$\overline{\theta}_j \doteq \max_{\theta \in \mathscr{D}_\theta} \theta_j, \tag{22.37}$$

can be computed finding the global optimal solution to the constrained optimisation problems (22.36) and (22.37). Because $\mathscr{D}_\theta$ is a nonconvex set defined by nonlinear inequalities in the variables θ, η_t and δx_t, numerical optimisation tools cannot be employed to solve problems (22.36) and (22.37) because they can trap in local minima/maxima, which may prevent the computed uncertainty intervals from containing the true parameter θ_j. One possible solution to overcome this problem is to relax (22.36) and (22.37) to convex problems to obtain a lower (upper) bound of $\underline{\theta}_j$ ($\overline{\theta}_j$).

In paper [6] the technique presented in [4], which provides a polytopic outer approximation of the FPS $\mathscr{D}_\theta$, is used to derive relaxed parameter uncertainty intervals through the solution of linear programming problems. In this Section, we exploit the algorithm for the computation of the PUIs (22.35) presented in [5], which is based on the approximation of the original optimisation problems (22.36) and (22.37) by a hierarchy of convex LMI relaxations. Relaxed parameter uncertainty intervals obtained through the application of such a technique are guaranteed to be less conservative than those computed in [6] and to contain the true unknown parameter θ_j. Besides, the computed relaxed bounds are guaranteed to converge monotonically to the tight ones defined in (22.36) and (22.37) as the number of successive LMI relaxations, the relaxation order δ, increases (see [5] for details).

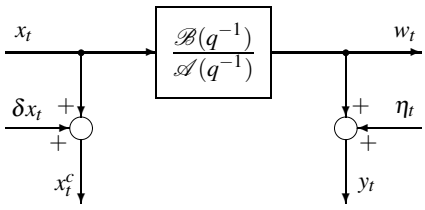

Fig. 22.4: Errors-in-variables basic setup for linear dynamic system

22.5 A Simulated Example

In this section we illustrate the presented parameter bounding procedure through a numerical example. The simulated system is characterised by a linear block with $\mathscr{A}(q^{-1}) = (1 - 0.76q^{-1} + 0.82q^{-2})$, $\mathscr{B}(q^{-1}) = (2.15q^{-1} - 1.09q^{-2})$ and a non-symmetric backlash with $m_l = 0.25$, $m_r = 0.26$, $c_l = 0.0628$, $c_r = 0.0489$. Thus, the true parameters vectors are $\gamma = [m_l \ c_l \ m_r \ c_r]^{\mathrm{T}} = [0.25 \ 0.0628 \ 0.26 \ 0.0489]^{\mathrm{T}}$ and $\theta = [a_1 \ a_2 \ b_1 \ b_2]^{\mathrm{T}} = [-0.76 \, 0.82 \ 2.15 \ -1.09]^{\mathrm{T}}$. It must be pointed out that the backlash parameters are realistically chosen. In fact, we consider the parameters of a real world precision gearbox which features a gear ratio equal to 0.25 and a deadzone as large as 0.0524rad ($\approx 3^o$) and simulate a possible fictitious non-symmetric backlash with gear ratio $m_l = 0.25$, $m_r = 0.26$ and deadzone $c_l = 0.0628$ ($\approx 3.6^o$), $c_r = 0.0489$ ($\approx 2.8^o$). Bounded absolute output errors are considered when simulating the collection of both steady state data $\{\bar{u}_s, \bar{y}_s\}$, and transient sequence $\{u_t, y_t\}$. Uncertainties $\bar{\eta}_s$ and η_t are random sequences belonging to the uniform

Table 22.1: Nonlinear block parameters evaluation: central estimates (γ_j^c), parameter bounds (γ_j^{min}, γ_j^{max}) and parameter uncertainty bounds $\Delta\gamma_j$

$\Delta\eta$	$\overline{SNR}$ (db)	γ_j	True Value	γ_j^{min}	γ_j^c	γ_j^{max}	$\Delta\gamma_j$
0.005	54	m_l	0.2500	0.2500	0.2500	0.2500	0.0000
		c_l	0.0628	0.0624	0.0628	0.0633	0.0005
		m_r	0.2600	0.2600	0.2600	0.2600	0.0000
		c_r	0.0489	0.0484	0.0489	0.0493	0.0004
0.02	42	m_l	0.25000	0.2496	0.2499	0.2503	0.0003
		c_l	0.06280	0.0512	0.0602	0.0693	0.0090
		m_r	0.26000	0.2596	0.2599	0.2603	0.0003
		c_r	0.04890	0.0377	0.0464	0.0550	0.0087
0.05	34	m_l	0.2500	0.2493	0.2501	0.2509	0.0008
		c_l	0.0628	0.0576	0.0649	0.0722	0.0073
		m_r	0.2600	0.2593	0.2601	0.2609	0.0008
		c_r	0.0489	0.0438	0.0509	0.0579	0.0070
0.15	25	m_l	0.2500	0.2488	0.2495	0.2503	0.0007
		c_l	0.06280	0.0504	0.0661	0.0818	0.0157
		m_r	0.2600	0.2588	0.2595	0.2603	0.0007
		c_r	0.04890	0.0369	0.0520	0.0671	0.0151
0.2	22	m_l	0.25000	0.2493	0.2503	0.2512	0.0009
		c_l	0.06280	0.0444	0.0626	0.0809	0.0182
		m_r	0.26000	0.2593	0.2603	0.2612	0.0009
		c_r	0.04890	0.0311	0.0487	0.0662	0.0175
0.3	18	m_l	0.25000	0.2490	0.2504	0.2518	0.0014
		c_l	0.06280	0.0352	0.0625	0.0898	0.0273
		m_r	0.26000	0.2590	0.2604	0.2618	0.0014
		c_r	0.04890	0.0223	0.0486	0.0749	0.0263

Table 22.2: Linear block parameters evaluation: central estimates (θ_j^c), parameter bounds (θ_j^{min}, θ_j^{max}) and parameter uncertainty bounds $\Delta\theta_j$ for $N = 100$

$\Delta\eta$	SNR (db)	θ_j	True Value	θ_j^{min}	θ_j^c	θ_j^{max}	$\Delta\theta_j$
0.005	50	a_1	-0.7600	-0.7605	-0.7600	-0.7596	0.0004
		a_2	0.8200	0.8196	0.8201	0.8205	0.0004
		b_1	2.1500	2.1470	2.1503	2.1535	0.0033
		b_2	-1.0900	-1.0943	-1.0906	-1.0860	0.0037
0.02	37	a_1	-0.7600	-0.7666	-0.7594	-0.7522	0.0072
		a_2	0.8200	0.8152	0.8205	0.8259	0.0054
		b_1	2.1500	2.1187	2.1506	2.1825	0.0319
		b_2	-1.0900	-1.1283	-1.0931	-1.0580	0.0352
0.05	29	a_1	-0.7600	-0.7664	-0.7601	-0.7539	0.0063
		a_2	0.8200	0.8142	0.8191	0.8240	0.0049
		b_1	2.1500	2.1201	2.1581	2.1960	0.0380
		b_2	-1.0900	-1.1461	-1.1005	-1.0550	0.0455
0.15	19	a_1	-0.7600	-0.7703	-0.760	-0.7497	0.0103
		a_2	0.8200	0.8050	0.8206	0.8353	0.0147
		b_1	2.1500	2.0725	2.1582	2.2439	0.0857
		b_2	-1.0900	-1.1953	-1.0985	-1.0017	0.0968
0.2	17	a_1	-0.7600	-0.7814	-0.7610	-0.7405	0.0204
		a_2	0.8200	0.8015	0.8224	0.8433	0.0209
		b_1	2.1500	2.0324	2.1680	2.3036	0.1356
		b_2	-1.0900	-1.2712	-1.1176	-0.9639	0.1537
0.3	14	a_1	-0.7600	-0.7933	-0.7606	-0.7278	0.0328
		a_2	0.8200	0.7914	0.8240	0.8567	0.0327
		b_1	2.1500	1.9652	2.1679	2.3707	0.2027
		b_2	-1.0900	-1.3676	-1.1346	-0.9016	0.2330

distributions $U[-\Delta\bar{\eta}_s, +\Delta\bar{\eta}_s]$ and $U[-\Delta\eta_t, +\Delta\eta_t]$, respectively. Bounds on steady-state and transient output measurement errors are supposed to have the same value, *i.e.*, $\Delta\bar{\eta}_s = \Delta\eta_t \doteq \Delta\eta$. The numerical example is performed for six different values of $\Delta\eta$. From the simulated steady-state data $\{\bar{w}_s, \bar{\eta}_s\}$ and the transient sequence $\{w_t, \eta_t\}$, the signal to noise rations $\overline{SNR}$ and SNR are evaluated, respectively, as

$$\overline{SNR} \doteq 10\log\left\{\sum_{s=1}^{M}\bar{w}_s^2 \Big/ \sum_{s=1}^{M}\bar{\eta}_s^2\right\}, \tag{22.38}$$

$$SNR \doteq 10\log\left\{\sum_{t=1}^{N} w_t^2 \Big/ \sum_{t=1}^{N}\eta_t^2\right\}. \tag{22.39}$$

For a given $\Delta\eta$, the length of steady-state and the transient data are $M = 50$ and $N = [100, 300]$ respectively. Parameters bounds of the linear system are computed

Table 22.3: Linear block parameters evaluation: central estimates (θ_j^c), parameter bounds (θ_j^{min}, θ_j^{max}) and parameter uncertainty bounds $\Delta\theta_j$ for $N = 300$

$\Delta\eta$	SNR (db)	θ_j	True Value	θ_j^{min}	θ_j^c	θ_j^{max}	$\Delta\theta_j$
0.005	50	a_1	-0.7600	-0.7603	-0.7600	-0.7598	0.0002
		a_2	0.8200	0.8196	0.8200	0.8204	0.0004
		b_1	2.1500	2.1464	2.1494	2.1525	0.0030
		b_2	-1.0900	-1.0924	-1.0892	-1.0861	0.0031
0.02	38	a_1	-0.7600	-0.7643	-0.7598	-0.7552	0.0045
		a_2	0.8200	0.8158	0.8202	0.8247	0.0044
		b_1	2.1500	2.1135	2.1435	2.1734	0.0300
		b_2	-1.0900	-1.1145	-1.0832	-1.0519	0.0313
0.05	30	a_1	-0.7600	-0.7641	-0.7597	-0.7552	0.0045
		a_2	0.8200	0.8153	0.8200	0.8246	0.0047
		b_1	2.1500	2.1266	2.1559	2.1853	0.0294
		b_2	-1.0900	-1.1273	-1.0964	-1.0655	0.0309
0.15	20	a_1	-0.7600	-0.7708	-0.7600	-0.7493	0.0107
		a_2	0.8200	0.8110	0.8213	0.8315	0.0102
		b_1	2.1500	2.0897	2.1599	2.2300	0.0701
		b_2	-1.0900	-1.1782	-1.0993	-1.0203	0.0790
0.2	18	a_1	-0.7600	-0.7721	-0.7605	-0.7488	0.0116
		a_2	0.8200	0.8034	0.8216	0.8398	0.0182
		b_1	2.1500	1.9965	2.1302	2.2638	0.1336
		b_2	-1.0900	-1.2069	-1.0651	-0.9233	0.1418
0.3	14	a_1	-0.7600	-0.7794	-0.7605	-0.7416	0.0189
		a_2	0.8200	0.7942	0.8226	0.8510	0.0284
		b_1	2.1500	1.9154	2.1234	2.3314	0.2080
		b_2	-1.0900	-1.2735	-1.0540	-0.8345	0.2195

through the LMI-based procedure proposed in Section 22.4, for an LMI relaxation order δ equal to 2. Results on the backlash parameters evaluation are reported in Table 22.1, while Table 22.2 and Table 22.3 show results on the linear block parameters estimation for a transient-data sequence length N equal to 100 and 300, respectively.

From Tables 22.1,22.2 and 22.3 it can be noted that the true parameters γ_j and θ_j belong to the computed intervals $\left[\gamma_j^{min},\ \gamma_j^{max}\right]$ and $\left[\theta_j^{min},\ \theta_j^{max}\right]$ respectively, for $j = 1,\ldots,4$. It must be pointed out that, although in principle the estimation algorithm is not guaranteed to provide tight bounds on the parameters of the linear block for a finite value of the relaxation order δ, in practice satisfactory bounds on the parameters θ are obtained also for low signals to noise ratio ($SNR < 20$ db) and for a small number of experimental measurements ($N = 100$).

22.6 Conclusion

A two stage procedure for bounding the parameters of a single-input single-output Hammerstein system, where the nonlinear block is a backlash and the output measurements are corrupted by bounded noise, is presented in this chapter. The proposed approach is based on the selection of the input signal in order to decouple the nonlinear and the linear block parameters. In the first stage, a set of square wave input signals with different amplitudes is applied and the corresponding steady-state output samples are collected, from which the characterisation of the backlash feasible parameter set is derived, thanks to the fact that in steady-state operating conditions the input-output mapping does not depend on the linear block. On the basis of the derived backlash feasible parameter set, parameter uncertainty intervals are evaluated by computing the global optima solutions to nonconvex optimisation problems. In the second stage, a method for computing bounds on the unmeasurable inner signal is presented when a pseudo random binary signal is applied to the system. The obtained inner signal bounds, together with output noisy measurements, are used to estimate the linear block parameters through the solution of a suitable errors-in-variables identification scheme. Recent results on relaxation techniques based on linear matrix inequalities are profitably used to compute the linear block parameter uncertainty intervals, which are guaranteed to converge monotonically to the tight ones as the relaxation order increases. The effectiveness of the procedure discussed in this chapter is shown through a simulated example, where satisfactory parameters bounds are obtained also for a small number of experimental data and in the presence of low signal to noise ratios.

Appendix

In this appendix a procedure for the computation of vertices and active constraints defining the feasible parameter set $\mathscr{D}_\gamma^l$ is presented. The following additional symbols and quantities are introduced: H_L is a list of active constraints boundaries, that is, each element $H_L(k)$ of the list is an active constraint boundary; the expression $X \leftarrow \{z\}$ means that the element z is included in the set or list X; $\mathscr{D}_\gamma^l(s)$ is the set of the backlash parameters that are consistent with the first s measurement, the error bound and the assumed backlash model structure. A formal description of $\mathscr{D}_\gamma^l(s)$ is:

$$\mathscr{D}_\gamma^l(s) \doteq \left\{(m_l, c_l) \in \mathbb{R}_+^2 : \bar{y}_j = m_l(\bar{u}_j - c_l) + \bar{\eta}_j, \mid \bar{\eta}_j \mid \leq \Delta\bar{\eta}_j; \;\; j = 1, \ldots, s\right\}. \tag{22.40}$$

The proposed procedure, Algorithm 22.1 below, works in four stages. First, the active constraints boundaries and the vertices of the set $\mathscr{D}_\gamma^l$ are characterised exploiting Definitions 1, 3, 5 and 6. Then, for each new measurement $\overline{u}_s$, the intersections among the constraints boundaries $h^+(\overline{u}_s)$ and $h^-(\overline{u}_s)$ and the active constraints boundaries contained in the list H_L are computed; these intersections are temporarily included in the set $\mathscr{V}(\mathscr{D}_\gamma^l)$; the constraints boundaries $h^+(\overline{u}_s)$ and $h^-(\overline{u}_s)$ are included in the list H_L. Further, vertices of $\mathscr{D}_\gamma^l(s)$ are obtained rejecting the constraints

Algorithm 22.1: Computation of vertices and active constraints of $\mathscr{D}_\gamma^l$

```
1. begin
2. V(D_γ^l) ← {h+(ū1) ⋂ h+(ū1)}.
3. V(D_γ^l) ← {h+(ū1) ⋂ h−(ū2)}.
4. V(D_γ^l) ← {h−(ū1) ⋂ h+(ū2)}.
5. V(D_γ^l) ← {h−(ū1) ⋂ h−(ū2)}.
6. H_L ← {h+(ū1), h+(ū2), h−(ū1), h−(ū2)}.
7. for s = 3 : 1 : M
8.         L = length(H_L);
9.         q = 0;
10.        for z = 1 : 1 : L
11.                V(D_γ^l) ← {h+(ū_s) ⋂ H_L(z)}.
12.          if h+(ū_s) ∉ H_L then
13.                H_L ← {h+(ū_s)}.
14.          end if
15.                V(D_γ^l) ← {h−(ū_s) ⋂ H_L(z)}.
16.          if h−(ū_s) ∉ H_L then
17.                H_L ← {h−(ū_s)}.
18.          end if
19.        end for
20.        V(D_γ^l) = {V(D_γ^l) ⋂ D_γ^l(s)}.
21.        for k=1:1:length(H_L)
22.          if ∃ j≠k : {H_L(k) ⋂ H_L(j)} ∈ V(D_γ^l) then
23.                H_aux(q) = H_L(k).
24.                q = q + 1.
24.          end if
25.        end for
26. H_L = H_aux.
27. end for
28. return H_L.
29. return V(D_γ^l).
30. end
```

boundaries intersections that do not satisfy all the constraints generated by the first s measurements, which implicitly define $\mathscr{D}_\gamma^l(s)$. Finally, H_L is updated retaining only the constraints boundaries whose intersection with each other is a vertex of $\mathscr{D}_\gamma^l(s)$.

References

1. Bai, E.W.: Identification of linear systems with hard input nonlinearities of known structure. Automatica 38, 853–860 (2002)
2. Bai, E.W.: Decoupling the linear and nonlinear parts in Hammerstein model identification. Automatica 40(4), 671–676 (2004)
3. Bapat, C.N., Popplewell, N., McLachlan, K.: Stable periodic motions of an impact-pair. Journal of Sound and Vibration 87, 19–40 (1983)

4. Cerone, V.: Parameter bounds for armax models from records with bounded errors in variables. Int. J. Control 57(1), 225–235 (1993)
5. Cerone, V., Piga, D., Regruto, D.: Set-membership EIV identification through LMI relaxation techniques. In: Proc. of American Control Conference, Baltimore, Maryland, USA (2010)
6. Cerone, V., Regruto, D.: Bounding the parameters of linear systems with input backlash. IEEE Trans. Automatic Control 52(3), 531–536 (2007)
7. Corradini, M.L., Orlando, G., Parlangeli, G.: A VSC approach for the robust stabilization of nonlinear plants with uncertain nonsmooth actuator nonlinearities — A unified framework. IEEE Trans. Automatic Control 49(5), 807–813 (2004)
8. Giri, F., Rochdi, Y., Chaoui, F.Z., Brouri, A.: Identification of hammerstein systems in presence of hysteresis-backlash and hysteresis-relay nonlinearities. Automatica 44(3), 767–775 (2008)
9. Kalafatis, A.D., Wang, L., Cluett, W.R.: Identification of Wiener-type nonlinear systems in a noisy enviroment. Int. J. Control 66(6), 923–941 (1997)
10. Krzyżak, A.: Identification of nonlinear block-oriented systems by the recursive kernel estimate. Int. J. Franklin Inst. 330(3), 605–627 (1993)
11. Lang, Z.Q.: Controller design oriented model identification method for Hammerstein system. Automatica 29(3), 767–771 (1993)
12. Lang, Z.Q.: A nonparametric polynomial identification algorithm for the Hammerstein system. IEEE Trans. Automatic Control 42(10), 1435–1441 (1997)
13. Ljung, L.: System Identification, Theory for the User. Prentince Hall, Upper Saddle River (1999)
14. Milanese, M., Norton, J., Piet-Lahanier, H., Walter, E. (eds.): Bounding approaches to system identification. Plenum Press, New York (1996)
15. Milanese, M., Vicino, A.: Optimal estimation theory for dynamic sistems with set membership uncertainty: an overview. Automatica 27(6), 997–1009 (1991)
16. Ninness, B., Gibson, S.: Quantifying the accuracy of Hammerstein model estimation. Automatica 38, 2037–2051 (2002)
17. Nordin, M., Gutman, P.O.: Controlling mechanical systems with backlash — a survey. Automatica 38, 1633–1649 (2002)
18. Söderström, T., Stoica, P.: System Identification. Prentice-Hall, Upper Saddle River (1989)
19. Stoica, P., Söderström, T.: Instrumental-variable methods for identification of Hammerstein systems. Int. J. Control 35(3), 459–476 (1982)
20. Sun, L., Liu, W., Sano, A.: Identification of a dynamical system with input nonlinearity. IEE Proc. Part D 146(1), 41–51 (1999)
21. Tao, G., Canudas de Wit, C.A.: Special issue on adaptive systems with non-smooth nonlinearities. Int. J. of Adapt. Control & Sign. Proces. 11(1) (1997)
22. Tao, G., Kokotovic, P.V.: Adaptive control of systems with actuator and sensor nonlinearities. Wiley, New York (1996)
23. Vörös, J.: Modeling and identification of systems with backlash. Automatica 46(2), 369–374 (2010)
24. Walter, E., Piet-Lahanier, H.: Estimation of parameter bounds from bounded-error data: a survey. Mathematics and Computers in simulation 32, 449–468 (1990)